Backflow Structure of Steady and Unsteady Separating Turbulent Boundary Layers

Naval K. Agarwal* and Roger L. Simpson†
Virginia Polytechnic Institute and State University, Blacksburg, Virginia 24061

Recent LDA measurements in unsteady separating turbulent boundary layers by the authors have revealed some new information on the phase-ensemble-averaged backflow behavior. In the large-amplitude unsteady flows studied, very large backflow velocities exist in the detached flow at some phases of the oscillation cycle, in some cases even greater than the freestream velocity. The Reynolds shearing stress and turbulence-energy production near the wall in the backflow region are not negligible at these phases. Under such conditions, Simpson's backflow velocity profile model is not applicable, and a normal turbulent boundary-layer type of structure appears to be present in the phase-ensemble-averaged near-wall backflow. These new features of backflow are discussed, and a new concept of a "re-entrainment velocity" of the backflow into the outer region downstream flow is introduced.

Nomenclature

A = constant in Eq. (1)
C_1, C_2 = constants
c = length of converging-diverging portion of test section, 4.9 m
$\hat{C}_f'$ = $\hat{\tau}_\omega/(\frac{1}{2}\rho\hat{U}_N^2)$, local skin-friction coefficient for the backflow
$\frac{dp}{dx}$ = streamwise pressure gradient
f = frequency of oscillation, Hz
$\hat{H}$ = backflow shape factor = $\hat{\delta}*/\hat{\theta}_N$
k = $\omega c/2\bar{U}_{ei}$, reduced frequency of the flow
$\hat{\ell}$ = mixing length
$\hat{M}$ = distance from wall to maximum-$\rho\hat{u}v$ location in boundary layer
$\hat{N}$ = distance from wall to maximum velocity in phase-ensemble-averaged backflow velocity profile
$\hat{N}'$ = distance from wall to $\partial\hat{U}/\partial y = 0$ location in phase-ensemble-averaged backflow velocity profile
R = $(\hat{U}_{ei\,\max} - \hat{U}_{ei\,\min})/2\bar{U}_{ei}$
$Re_{\hat{\theta}N}$ = $\hat{U}_N\hat{\theta}_N/\nu$, momentum thickness Reynolds number in the backflow
$\hat{q}^2$ = $(\hat{u}^2 + \hat{v}^2 + \hat{w}^2)$
t = time
$\hat{U}, \hat{V}$ = phase-ensemble-averaged velocities in x, y directions, respectively
u, v, w = turbulent fluctuations in x, y, and z directions, respectively
$\hat{U}_e$ = phase-ensemble-averaged freestream velocity
$\bar{U}_{ei}$ = mean test section entrance time-averaged freestream velocity
$\hat{U}_N$ = maximum phase-ensemble-averaged backflow velocity
$\hat{U}_N'$ = phase-ensemble-averaged backflow velocity at a distance $\hat{N}'$ from the wall
$\hat{U}_\tau$ = $(\hat{\tau}_w/\rho)^{1/2}$, shear velocity
$\hat{U}^+$ = $\hat{U}/\hat{U}_\tau$
$\hat{u}^2, \hat{v}^2, \hat{w}^2$ = phase-ensemble-averaged mean square values of u, v, *and* w, respectively
$-\rho\hat{u}v$ = phase-ensemble-averaged Reynolds shear stress
$\hat{V}_{re}$ = phase-ensemble-averaged re-entrainment velocity
x, y, z = streamwise from leading edge, normal and spanwise coordinates
X_0 = streamwise location of flow detachment from the wall
$\hat{y}^+$ = $y\hat{U}_\tau/\nu$
$\hat{\gamma}_{pu}$ = forward flow fraction
$\hat{\delta}$ = y, where $\hat{U} = 0.99\hat{U}_e$
$\hat{\delta}_{0.995}$ = y, where $\hat{U} = 0.995\hat{U}_e$
$\hat{\delta}_b$ = backflow thickness
$\hat{\delta}*$ = $\int_0^{\hat{N}} [1 - (\hat{U}/\hat{U}_N)]dy$ = displacement thickness in the backflow
$\hat{\theta}_N$ = $\int_0^{\hat{N}} (\hat{U}/\hat{U}_N)\,[1 - (\hat{U}/\hat{U}_N)]dy$ = moment = thickness in the backflow
κ = von Kármán constant, 0.41
ν = kinematic viscosity
ρ = density
$\hat{\tau}_{max}$ = maximum value of shear stress in the boundary layer
$\hat{\tau}_w$ = wall shear stress
ω = $2\pi f$

Subscripts
e = freestream or conditions outside shear flow
i = freestream entrance conditions
max, min = maximum and minimum values

Introduction

TURBULENT separated flows are of considerable interest because of their practical importance in many applications. Until recent years, little reliable experimental information was available on the structure downstream of separation in such flows, especially for the near-wall backflow region. Pitot tube and hot-wire anemometry techniques in separated flow are limited by the fact that such probes produce directionally ambiguous results.[1-3] With the invention of laser-Doppler and pulsed-wire anemometry, a number of researchers have studied the near-wall region of separated flows, obtaining more reliable results. However, in many experiments, the thickness of the backflow region and mean backflow velocities were too small for detailed measurements.

Presented as Paper 89-0567 at the AIAA 27th Aerospace Sciences Meeting, Reno, NV, January 12-15, 1989.

*Visiting Assistant Professor, Department of Aerospace and Ocean Engineering; presently Research Scientist, Analytical Services and Materials, Inc., Hampton, VA. Senior Member AIAA.

†Jack E. Cowling Professor, Department of Aerospace and Ocean Engineering. Associate Fellow AIAA.

Simpson[4] proposed a correlation to fit low-velocity ($\hat{U}_N/\hat{U}_e < 0.25$) backflow profiles when $\hat{\tau}_\omega = 0$, and suggested that, in the phase-ensemble-averaged backflow, $\hat{U}/|\hat{U}_N|$ is a function of $(y/\hat{N})$.[5-8] (Phase-ensemble-averaged quantities were obtained by ensemble-averaging the measurements for that phase over at least 200 cycles. Here we denote phase-ensemble-averaged quantities by a caret above the symbol). The equation

$$\frac{\hat{U}}{|\hat{U}_N|} = A\left(\frac{y}{\hat{N}} - \ell n\left|\frac{y}{\hat{N}}\right| - 1\right) - 1 \qquad (1)$$

describes the velocity profile of the middle region of the phase-ensemble-averaged backflow, $0.02 < y/\hat{N} < 1$, downstream of detachment ($\hat{\gamma}_{pu} < \frac{1}{2}$ near the wall) and correlates the data of Simpson et al.[5-9] and Dianat and Castro[10] in this region. Farther away from the wall, this equation does not describe the velocity profile since the outer backflow region is influenced strongly by the outer region flow. Nearest the wall ($y/\hat{N} < 0.02$), the viscous sublayer can be described by[4]

$$\frac{\hat{U}}{|\hat{U}_N|} = -C_1\left(\frac{y}{\hat{N}}\right) + \frac{P_1}{2}\left(\frac{y}{\hat{N}}\right)^2 \qquad (2)$$

where $P_1 = (\hat{N}^2/\rho\nu|\hat{U}_N|)\,(dp/dx)$ and C_1 is a constant. The pressure gradient term is relatively small for these flows.[4] The viscous sublayer joins Eq. (1) tangentially at $y/\hat{N} = 0.035$ with a C_1 of 8.25.

However, as discussed in this paper, Simpson's backflow mean velocity profile model is applicable only in low-velocity backflow cases, where the Reynolds shearing stress near the wall is negligible. In such cases, turbulence-energy production near the wall is negligible and hence turbulence-energy diffusion toward the wall is responsible for the turbulence energy dissipated near the wall.[5,6]

Recent LDA measurements in three unsteady separating turbulent boundary layers by the authors have revealed some new information on the phase-ensembled-averaged backflow behavior, which is presented here.[11-15] In the two large-amplitude flows studied, very large phase-ensembled-averaged backflow velocities have been measured. Substantial turbulence-energy near the wall is produced at these phases of the cycle (with large backflow velocities), and Simpson's mean backflow velocity correlation is not applicable. In another unsteady flow with a diverging freestream, negligible turbulence-energy production near the wall exists, and Simpson's mean backflow velocity correlation is applicable very near to the wall. Detailed velocity and turbulence measurements for these flows are reported in Refs. 14 and 15, respectively, and are also contained in a technical report.[13]

Phase-ensembled-averaged backflow velocity profile data for these three unsteady flows and earlier measurements of Simpson et al.[5-9] in steady and unsteady separating boundary layers are examined here. In the large-amplitude flows at the phases of the oscillation cycle with substantial turbulence-energy production, the normal attached-flow law-of-the-wall velocity profiles appear to be valid in the backflow under some conditions. In another unsteady flow with a diverging freestream, very thick backflow is produced, and the mean backflow velocity shapes are quite different away from the wall.

These observations and conditions of applicability of Simpson's mean backflow velocity correlation and the law of the wall in the phase-ensembled-averaged mean backflow are discussed in this paper. Attention is also concentrated on the re-entrainment of flow from the backflow region into the outer region shear layer.

Description of Test Flows

Phase-ensemble-averaged backflow velocity results are presented for three unsteady separating turbulent boundary layers; two with large-amplitude unsteadiness (first harmonic amplitude/mean velocity ratio of 0.75 ($R = 0.63$ and 0.74) and reduced frequencies, $k = 0.61$ and 1.33, with f, the frequency of oscillations as 0.596 and 0.954 Hz, respectively) and another with a diverging freestream [first harmonic amplitude/mean velocity ratio of 0.12 ($R = 0.17$) and $k = 1.03$ with $f = 0.954$ Hz], hereafter called the "roof-damper flow." The wind tunnel, with a 8-m- long and 0.91-m-wide converging-diverging test section with boundary-layer control; the programmable-rotating blade damper for producing large-amplitude unsteadiness; and the hot-wire and laser anemometers used in these measurements have been described in detail in Refs 5-9 and 11-13.

Changes made in the diverging section to produce the roof-damper flow[13,15] are briefly described here. The rotating damper used downstream of the mainstream blower in large-amplitude experiments was fixed open, so that the flow at the entrance to the test section was almost steady. The roof of the diverging section was replaced by a mesh screen, which permitted part of the mainstream flow to be periodically diverted through the roof. A damper with 12 rotating blades mounted above this section controlled the phase and amplitude of the flow. A wooden piece 0.38 m long was placed over the roof to delay detachment. The wind-tunnel test section with these modifications is schematically shown in Fig. 1. The phase-ensemble-averaged freestream velocity distributions at approximately the test section throat (minimum cross-sectional area location) for the flows studied are shown in Fig. 2. Note the abrupt changes in freestream velocity distribution (40 deg $< \omega t <$ 70 deg) for the $k = 1.33$ flow as a result of a disturbance generated upstream.[13,14] These flows are described in detail in Refs. 13-15.

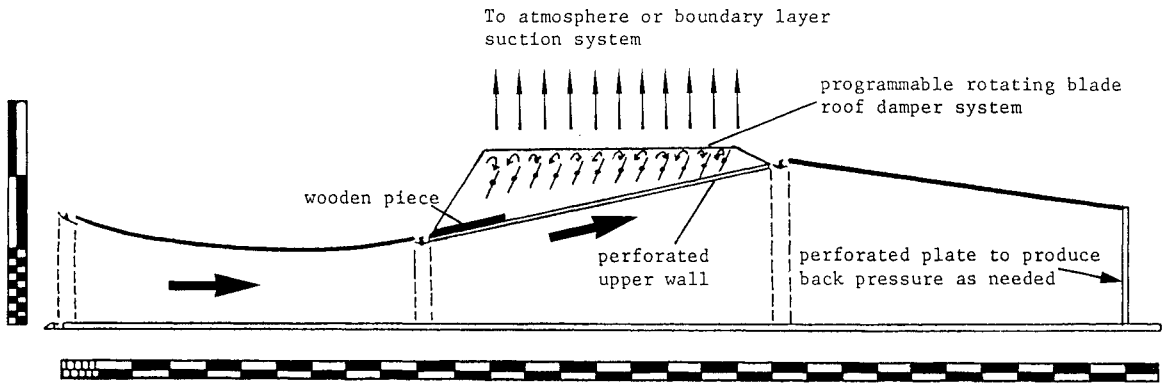

Fig. 1 Side view of the test section with modifications for $k = 1.03$ flow with roof damper. Major dimension on scale is 25 cm. Note baffle plate upstream of blunt leading edge on bottom test wall and side- and upper-wall jet boundary-layer control.

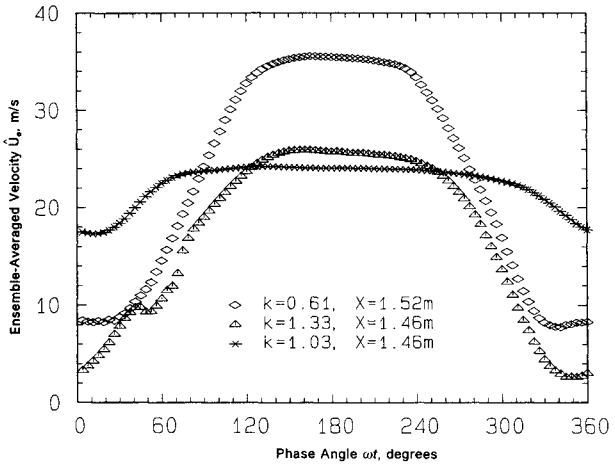

Fig. 2 Ensembled-averaged freestream velocity, $\hat{U}_e$ distributions.

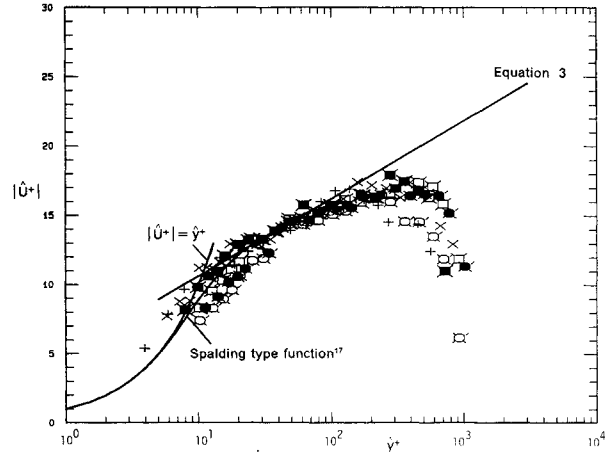

Fig. 3a Backflow velocity profiles plotted in law-of-the-wall coordinates, $|\hat{U}^+|$ vs $\hat{y}^+$, $X = 2.95$ m, $k = 0.61$ (large-amplitude) flow, at phases 315 deg $\leq \omega t \leq$ 30 deg: ($\times$, $\omega t = 15$ deg, $\hat{U}_N = 3.16$ m/s; + = 30 deg, 2.10 m/s; □ = 315 deg, 5.29 m/s; ■ = 330 deg, 5.96 m/s; □ = 345 deg, 5.50 m/s; ■ = 360 deg, 4.33 m/s).

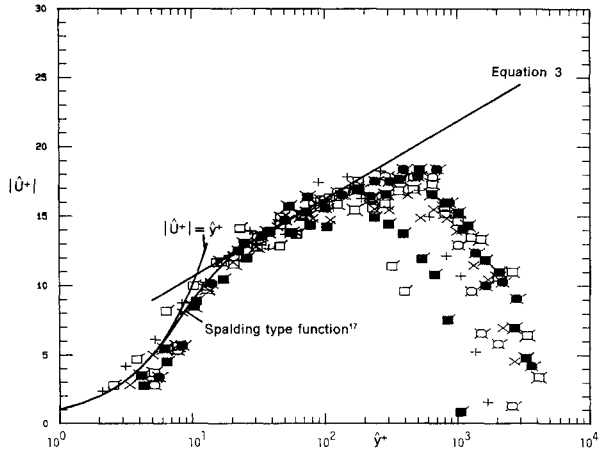

Fig. 3b Backflow velocity profiles plotted in law-of-the-wall coordinates, $|\hat{U}^+|$ vs $\hat{y}^+$, $X = 3.15$ m, $k = 0.61$ (large-amplitude) flow, at phases 285 deg $\leq \omega t \leq$ 30 deg: ($\times$, $\omega t = 15$ deg, $\hat{U}_N = 3.48$ m/s; + = 30 deg, 2.40 m/s; □ = 285 deg, 0.68 m/s; ■ = 300 deg, 4.00 m/s; □ = 315 deg, 5.77 m/s; ■ = 330 deg, 6.40 m/s; □ = 345 deg, 5.56 m/s; ■ = 360 deg, 4.72 m/s).

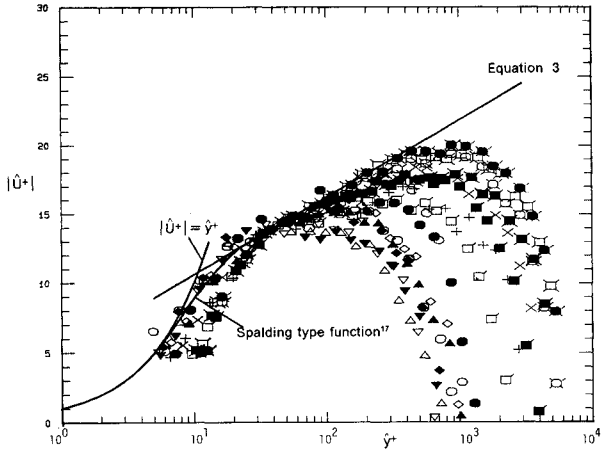

Fig. 3c Backflow velocity profiles plotted in law-of-the-wall coordinates, $|\hat{U}^+|$ vs $\hat{y}^+$, $X = 4.27$ m, $k = 0.61$ (large-amplitude) flow, at phases 165 deg $\leq \omega t \leq$ 45 deg: ($\times$, $\omega t = 15$ deg, $\hat{U}_N = 4.67$ m/s; + = 30 deg, 3.47 m/s; ○ = 45 deg, 1.81 m/s; △ = 165 deg, 2.57 m/s; ▲ = 180 deg, 3.28 m/s; ◇ = 195 deg, 3.18 m/s; ◆ = 210 deg, 2.84 m/s; ▽ = 225 deg, 2.39 m/s; ▼ = 240 deg, 2.38 m/s; ○ = 255 deg, 2.82 m/s; ● = 270 deg, 3.69 m/s; □ = 285 deg, 4.79 m/s; ■ = 300 deg, 6.11 m/s; □ = 315 deg, 7.50 m/s; ■ = 330 deg, 7.81 m/s; □ = 345 deg, 6.95 m/s; ■ = 360 deg, 5.70 m/s).

Phase-Ensemble-Averaged Velocity Profiles

The large-amplitude flows show some new features in the backflow that were not observed in moderate-amplitude flows (first harmonic amplitude/mean velocity ratio of 0.33 and k = 0.61, 0.90) studied earlier by Simpson et al.[7,8] using the same test facility. Low backflow velocities ($\hat{U}_N/\hat{U}_e \leq 0.3$) and nearly zero Reynolds shearing stress close to the wall were measured in these moderate-amplitude flows of Simpson et al.

Phase-ensemble-averaged backflow velocity profiles in the large-amplitude flows do not correlate with Simpson's model at most of the phases of the oscillation cycle. Thus, several other proposed models for backflow velocity profiles were examined. Adams and Johnston[16] suggested a velocity profile law of the type $\hat{U}/U_N = f(y,N,\nu)$ on the assumption that only the parameters $\hat{U}_N$, $\hat{N}$, and ν affect the flow structure. They obtained a fair collapse of their data in the backflow region using $\hat{U}/\hat{U}_N$ vs $f(\hat{U}_N/\nu\hat{N})^{1/2}$ coordinates. Simpson's backflow model expressed in terms of these coordinates produced a marginally better, but still unsatisfactory, collapse of the present large backflow velocity profiles.

Simpson[4] suggested that the $\hat{U}^+$ vs $\hat{y}^+$ type of law-of-the-wall scaling was not possible in the low-velocity backflow cases he examined because the law of-the-wall length scale $\nu/\hat{U}_\tau$ varies inversely with its velocity scale $\hat{U}_\tau$, whereas the measured length scale $\hat{N}$ and velocity scale $\hat{U}_N$ both increased with the streamwise distance. However, in the large-amplitude flows, $\hat{N}$ increases and $\hat{U}_N$ remains nearly constant. This feature and the significant turbulence-energy production near the wall,[13,14] which is as large as outer region production at some phases, suggest the possible existence of normal turbulent boundary-layer features near the wall and the possible applicability of the attached-flow law of the wall in the near-wall backflow. Very large backflow velocities in large-amplitude flows appear to be responsible for significant turbulence-energy production and nonzero Reynolds shearing stress near the wall.

Other evidence is that values of $\hat{U}_\tau$ calculated from the semilogarithmic relation

$$\hat{U}^+ = \frac{1}{\kappa} \ln \hat{y}^+ + 5.0 \qquad (3)$$

at $\hat{y}^+ = 30$ for the phases of the oscillation cycles with substantial turbulence-energy production close to the wall agree

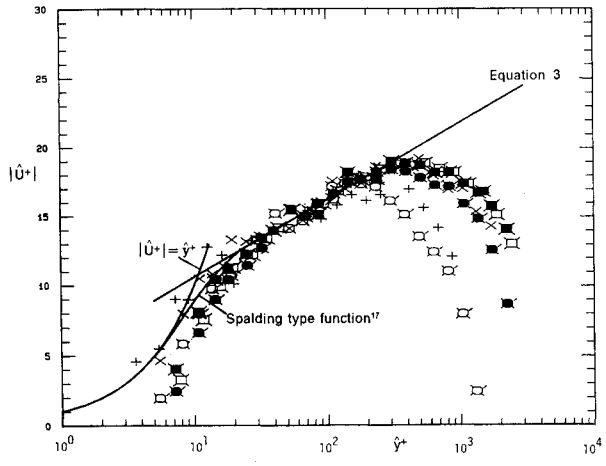

Fig. 4a Backflow velocity profiles plotted in law-of-the-wall coordinates, $|\hat{U}^+|$ vs $\hat{y}^+$, $X = 2.95$ m, $k = 1.33$ (large-amplitude) flow, at phases 315 deg $\leq \omega t \leq$ 30 deg: ($\times$, $\omega t = 15$ deg, $\hat{U}_N = 6.57$ m/s; + = 30 deg, 3.75 m/s; ⧈ = 315 deg, 5.90 m/s; ■ = 330 deg, 8.25 m/s; ⧈ = 345 deg, 9.22 m/s; ■ = 360 deg, 8.50 m/s).

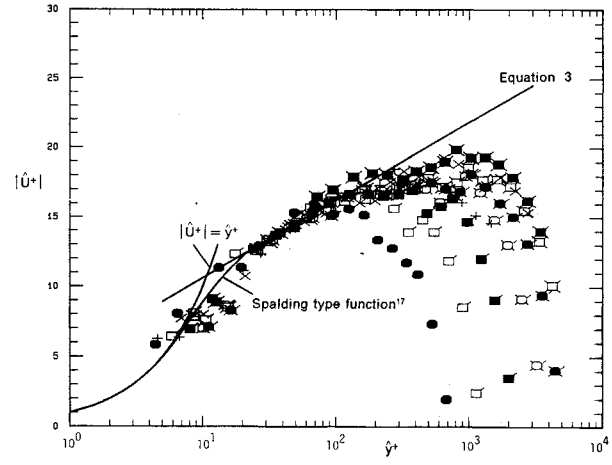

Fig. 4b Backflow velocity profiles plotted in law-of-the-wall coordinates, $|\hat{U}^+|$ vs $\hat{y}^+$, $X = 3.51$ m, $k = 1.33$ (large-amplitude) flow, at phases 270 deg $\leq \omega t \leq$ 30 deg: ($\times$, $\omega t = 15$ deg, $\hat{U}_N = 5.54$ m/s; + = 30 deg, 3.35 m/s; ● = 270 deg, 2.85 m/s; □ = 285 deg, 4.04 m/s; ■ = 300 deg, 5.55 m/s; ⧈ = 315 deg, 7.25 m/s; ■ = 330 deg, 8.06 m/s; ⧈ = 345 deg, 8.00 m/s; ■ = 360 deg, 7.01 m/s).

within experimental uncertainties with the measured values of $-\rho\hat{u}\hat{v}$ closest to the wall.[13,14] Phase-ensemble-averaged backflow velocities plotted in law-of-the-wall coordinates show similarity, and data appear to follow the law-of-the-wall profile, even in the $|\hat{U}^+| = \hat{y}^+$ sublayer, as shown in Figs. 3 and 4 for the phases with phase-ensemble-averaged backflow at $X = 2.95$ m, 3.51 m and 4.27 m, for $k = 0.61$ and 1.33 flows. Viscous sublayer, buffer layer, and semilogarithmic regions are shown by a solid line in these figures. In the buffer layer, a Spalding-type function is used.[17] A negative wake is clearly evident, and velocity profiles look very similar to a wall jet type of flow such as that studied by Saripalli and Simpson.[18] (With a limited amount of laser anemometer data, Patrick[19] also suggested that the law-of-the-wall profile may apply to the backflow, but he lacked data close to the wall.)

On the other hand, at some phases of the oscillation cycle where backflow velocities are low and turbulence-energy production close to the wall is negligible, Simpson's backflow correlation holds, e.g., as shown in Fig. 5 for the $k = 1.33$ flow at $X = 3.51$ m. Figure 5 shows that data closely follow Eq. (1) for $0.02 \leq y/\hat{N} \leq 1.0$. In the near-wall backflow $y/\hat{N} \leq 0.02$, where Reynolds shearing stress is negligible, the data

Fig. 4c Backflow velocity profiles plotted in law-of-the-wall coordinates, $|\hat{U}^+|$ vs $\hat{y}^+$, $X = 4.27$ m, $k = 1.33$ (large-amplitude) flow, at phases 255 deg $\leq \omega t \leq$ 60 deg: ($\times$, $\omega t = 15$ deg, $\hat{U}_N = 8.03$ m/s; + = 30 deg, 6.66 m/s; ○ = 45 deg, 5.00 m/s; * = 60 deg, 2.93 m/s; ○ = 255 deg, 4.18 m/s; ● = 270 deg, 5.25 m/s; □ = 285 deg, 5.70 m/s; ■ = 300 deg, 6.37 m/s; ⧈ = 315 deg, 6.91 m/s; ■ = 330 deg, 7.20 m/s; ⧈ = 345 deg, 7.60 m/s; ■ = 360 deg, 8.24 m/s).

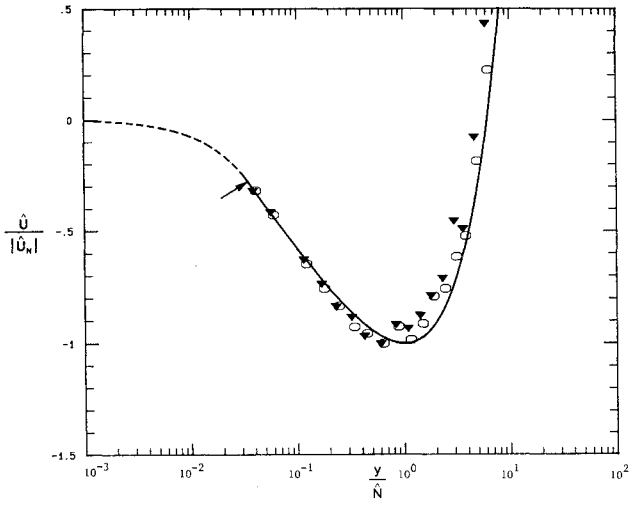

Fig. 5 Normalized backflow velocity profiles at $X = 3.51$ m, $k = 1.33$ (large-amplitude) flow, at the phases (beginning of detachment) where Simpson's backflow correlation is applicable; ▼, $\omega t = 240$ deg; ○, $\omega t = 255$ deg. Solid line is given by Eq. (1). Viscous sublayer, Eq. (2), shown by dotted line, meets tangentially with Eq. (1) at arrow.

follow the sublayer given by Eq. (2), as shown in Fig. 5. These are the phases where the flow just starts separating, with accompanying low values of $\hat{U}_N$ and $\hat{N}$.

For the $k = 1.03$ flow with the roof damper, backflow occurs downstream of $X = 3.01$ m at all the phases of the oscillation cycle, and moderate backflow velocities, $\hat{U}_N/\hat{U}_e \leq 0.3$ exist. The backflow thickness in this flow is very large compared to the large-amplitude flows. Negligible turbulence-energy production and Reynolds shearing stress are produced for all the phases close to the wall.[13,15] Outer backflow profile shapes for this flow are quite different (Fig. 6) than those observed in Refs. 5-9 and 12-14.

The phase-ensemble-averaged backflow velocity increases away from the wall, reaching a region of $(\partial\hat{U}/\partial y) = 0$ and then increasing again until it reaches a maximum backflow velocity, as shown in Fig. 6a for $X = 3.59$ m. This behavior is more pronounced at $X = 4.12$ m, as shown in Fig. 6b. A similar backflow velocity profile shape was observed by Adair and Horne[20] and Thompson and Whitelaw[21] for separated

flow over an airfoil flap. However, Adair and Horne did not have data close to the wall to compare with Simpson's correlation. The backflow thickness $\hat{N}'$ is chosen just at the beginning of the $(\partial\hat{U}/\partial y) = 0$ region. Simpson's correlation holds close to the wall for the phases of the cycle with backflow as shown in Figs. 6a and 6b at $X = 3.59$ and 4.12 m. In the present study and earlier studies by Simpson et al.[5,6,9] a good correlation with Eq. (1) exists with $A = 0.3$. However, Dianat and Castro[10] found that their pulsed-wire data were well described with $A = 0.235$. The reason for this difference is not clear.

Simpson's backflow model [Eq. (1)] does not describe the outer region of the backflow (Figs. 6a and 6b). In addition, there appears to be two different length scales in the inner and outer regions of the backflow that appear to govern the backflow turbulence behavior. Semilogarithmic profiles of $\hat{u}^2$ between inflection points suggest an overlap region between inner and outer velocity and length scales.[13-15] In an attempt to correlate the outer region backflow velocity, various length scales, e.g., $\hat{N}$, $\hat{N}'$, $\hat{\delta}$, and $\hat{M}$ were tried, but they did not correlate the outer backflow region for the large-amplitude and roof-damper flows.

Integral parameters based on the maximum phase-ensemble-averaged backflow velocity, $\hat{U}_N$, were calculated for large-amplitude and roof-damper flows and the steady and unsteady flows of Simpson et al.[5-9] All of these data plotted in $\hat{U}_N/\hat{U}_e$ vs $Re_{\hat{\theta}N}$ coordinates (Fig. 7) fall into two distinct regions: one for which Simpson's correlation holds (filled symbols) and the other to which the normal $|\hat{U}^+|$ vs $\hat{y}^+$ law of the wall appears to apply. The shapes of the mean backflow profiles close to the wall are substantially different in these two cases. For the cases for which Simpson's correlation holds, a shape parameter $\hat{H}$ has a value close to 1.8 whereas, in the other case, a value of 1.34–1.6 is obtained. It should be noted that the momentum thickness Reynolds number, $Re_{\hat{\theta}N}$ is more than about 200 when the law of the wall holds in the backflow.

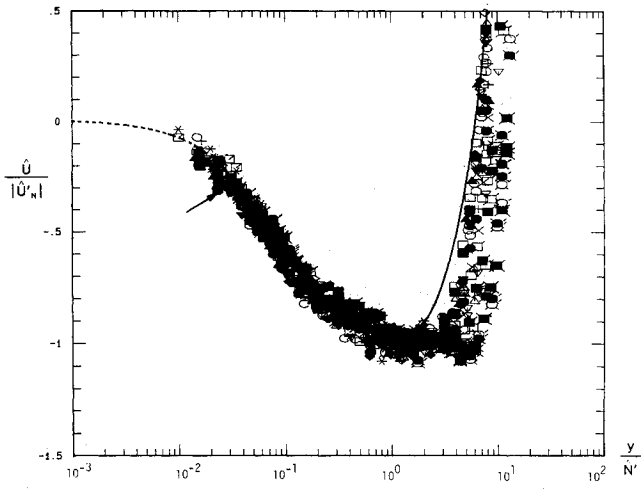

Fig. 6a Normalized backflow velocity profiles at $X = 3.59$ m, $k = 1.03$ flow with roof damper at phases 0 deg $\leq \omega t \leq$ 360 deg: (×, $\omega t = 15$ deg; + = 30 deg; ○ = 45 deg; * = 60 deg; ☐ = 75 deg; △ = 90 deg; ▽ = 105 deg; ⊖ = 120 deg; □ = 135 deg; ■ = 150 deg; △ = 165 deg; ▲ = 180 deg; ◇ = 195 deg; ◆ = 210 deg; ▽ = 225 deg; ▼ = 240 deg; ○ = 255 deg; ● = 270 deg; ☐ = 285 deg; ■ = 300 deg; ☐ = 315 deg; ■ = 330 deg; ☐ = 345 deg; ■ = 360 deg). Solid line is given by Eq. (1). Viscous sublayer, (Eq. 2), shown by dotted line, meets tangentially with Eq. (1) at arrow.

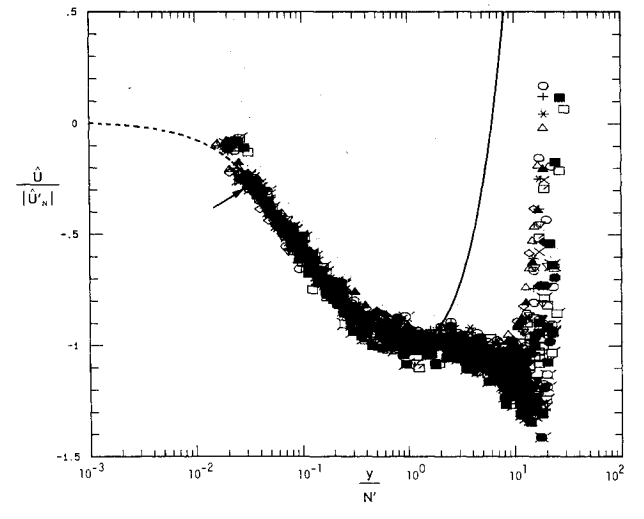

Fig. 6b Normalized backflow velocity profiles at $X = 4.12$ m, $k = 1.03$ flow with roof damper at phases 0 deg $\leq \omega t \leq$ 360 deg. Solid line is given by Eq. (1). Viscous sublayer, (Eq. 2), shown by dotted line, meets tangentially with Eq. (1) at arrow. Legend same as that for Fig. 6a.

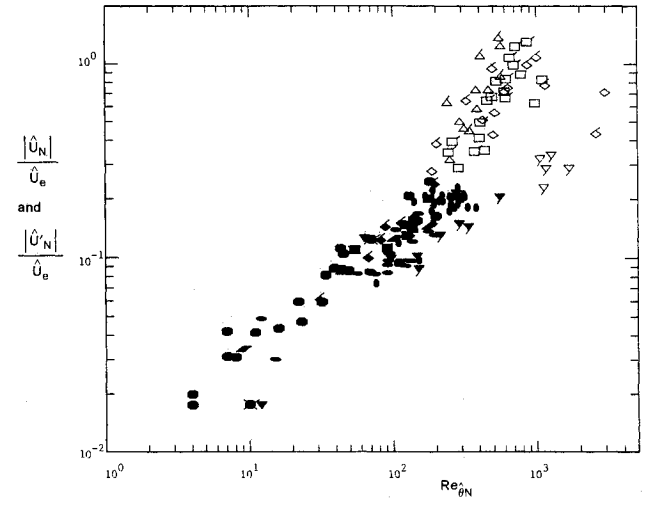

Fig. 7 $|\hat{U}_N|/\hat{U}_e$ vs $Re_{\hat{\theta}\hat{N}}$; △, $X = 2.95$ m, ◇ = 3.51 m, □ = 4.27 m, $k = 0.61$ (large-amplitude) flow; △ = 2.95 m, ◇ = 3.51 m, ☐ = 4.27 m $k = 1.33$ (large-amplitude) flow; ● = 3.28 m, ● = 3.54 m, $k = 1.03$ flow with roof damper; Simpson et al.[5]; ▽ ▼, Simpson et al.[7]; ●, Simpson et al.[8]; ▼, flow C, ■, flow D, Simpson et al.[9] Filled symbols where Eq. (1) and (2) hold. Open symbols where the law of the wall holds.

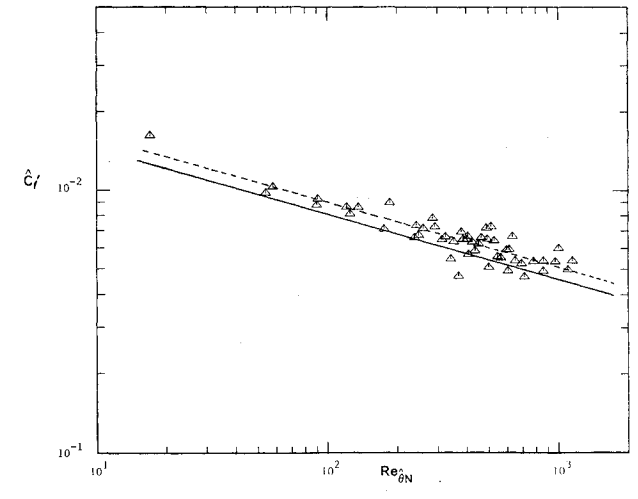

Fig. 8 $\hat{C}_f$ vs $Re_{\hat{\theta}\hat{N}}$; solid line given by Eq. (4) ($C_2 = 0.0256$); dashed line shows the effect of outer region turbulence.

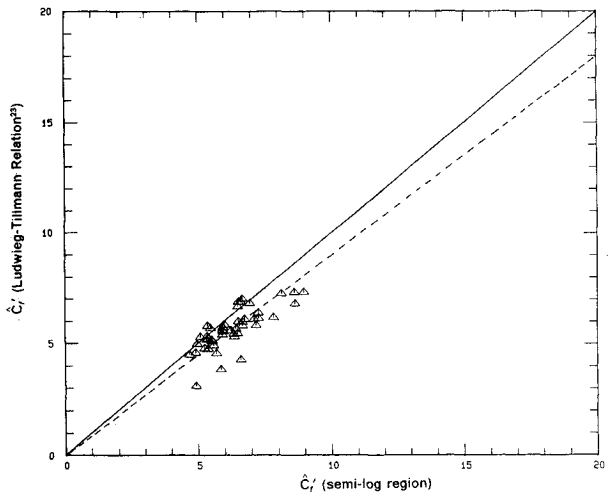

Fig. 9 Correlation between $\hat{C}_f'$ obtained from semilog region and $\hat{C}_f'$ obtained from Ludwieg-Tillmann relation[22] for $k = 0.61$ and $k = 1.33$ (large-amplitude) flows. Dashed line shows the effect of outer region turbulence.

We can define a local backflow skin-friction coefficient $\hat{C}_f'$ based on $\hat{U}_N$. For the cases for which the law-of-the-wall profile holds in the backflow, one would expect a universal relationship between $\hat{C}_f'$ and $Re_{\hat{\theta}N}$. $\hat{C}_f'$ data from the above-mentioned calculated $\hat{U}_\tau$ results suggest a relationship of the form (Fig. 8)

$$\hat{C}_f' = C_2 Re_{\hat{\theta}N}^{-1/4} \tag{4}$$

which is the same as that suggested with $C_2 = 0.0256$ for the friction coefficient in terms of a local momentum thickness Reynolds number for zero and mild favorable pressure gradient boundary layers.[17] Data in Fig. 8 are close to the line given by Eq. (4). Although there is some scatter in the data, they appear to be systematically above the line. Skin-friction coefficients calculated using the Ludwieg-Tillmann relation,[22] as shown in Fig. 9, are also slightly lower than those obtained from the semilogarithmic region in the backflow.

These slightly higher values of $\hat{C}_f'$ appear to be due to the influence of the larger-scale outer region turbulent flow on the near-wall backflow. Hancock and Bradshaw[23] studied the effect of freestream turbulence on skin-friction coefficients of attached turbulent boundary layers and found that they increased and $\hat{H}$ decreased with increasing freestream turbulence. Using the correlation results of Hancock and Bradshaw, $\hat{C}_f'$ in the present experiments should be about 10% higher than the solid line shown in Fig. 8 because of outer region turbulence. Experimental values of $\hat{C}_f'$ are about 10% higher than the line, indicating good agreement.

Re-Entrainment of the Backflow into the Outer Region Flow

At any given X location where there is mean backflow, the continuity equation requires that the velocity $\bar{V}$ at the $\bar{U} = 0$ line be given by

$$\bar{V}|_{\bar{U}=0} = -\frac{\mathrm{d}}{\mathrm{d}X}\left[\int_0^{\bar{\delta}_b(X)} \bar{U}\mathrm{d}y\right] \tag{5}$$

However, this relation is valid only for the steady flows. In the case of unsteady flow, the normal-to-the-wall flow velocity $\hat{V}$ at the $\hat{U} = 0$ line at a given time contributes backflow fluid that goes to increase the thickness of the backflow zone as well as to provide fluid to be transported to the outer region. Therefore, the velocity relative to the moving $\hat{U} = 0$ line will be given by $\bar{V}|_{\bar{U}=0} - (\partial\bar{\delta}_b/\partial t) = \hat{V}_{re}$ (refer to Fig. 10). Thus,

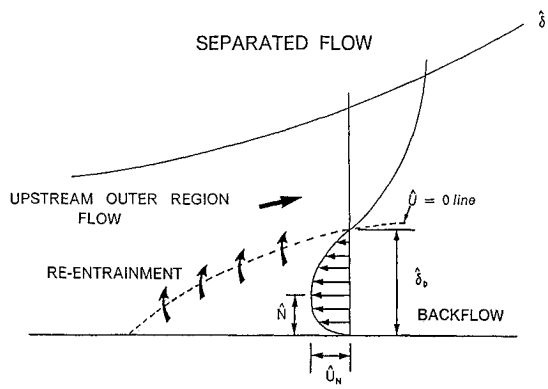

Fig. 10 A flow model showing the flow separation and re-entrainment of the backflow.

the unsteady continuity equation leads to

$$\hat{V}_{re} = \bar{V}|_{\bar{U}=0} - \frac{\partial\hat{\bar{\delta}}_b}{\partial t} = -\frac{\partial}{\partial X}\left[\int_0^{\hat{\delta}_b(X,t)} \hat{U}\mathrm{d}y\right] \tag{6}$$

$\hat{V}_{re}$ at a given X location is the phase-ensemble-averaged velocity of fluid that is re-entrained into the forward flow.

This equation also leads to

$$\int_{X_0}^{X} \hat{V}_{re}\mathrm{d}X = \int_{X_0}^{X}\left[\hat{V}|_{\hat{U}=0} - \frac{\partial\hat{\bar{\delta}}_b}{\partial t}\right]\mathrm{d}X = -\int_0^{\hat{\delta}_b(X)} \hat{U}\mathrm{d}y \tag{7}$$

when integrated from detachment at X_0 to a given X location downstream. This right-hand side is the total volumetric flow rate of the backflow at X. This also shows that this backflow mean flow rate at X is dependent on $\hat{V}|_{\hat{U}=0}$ and $(\partial\delta_b/\partial t)$ at all locations between detachment and a given X location.

The re-entrainment velocity $\hat{V}_{re}$ should be controlled by the outer region flow. Bradshaw et al.[24] suggest that $\hat{V}_{entrainment}$ scales on $(\hat{\tau}_{max}/\rho)^{1/2}$, which is the diffusion velocity for turbulence kinetic energy for the outer region turbulent/nonturbulent interface ($q^2 v = \hat{q}^2 \hat{V}_{entrainment}$). This suggested that perhaps the re-entrainment velocity $\hat{V}_{re}$ at $\hat{U} = 0$ scales on $(\hat{\tau}_{max}/\rho)^{1/2}$. However $\hat{V}_{re}/(\hat{\tau}_{max}/\rho)^{1/2}$ did not correlate the present data and the steady flows of Refs. 5 and 9.

East and Sawyer[25] suggest that

$$q^2 v = -0.4\hat{\ell}\frac{\mathrm{d}(\hat{q}^2)^{3/2}}{\mathrm{d}y} \tag{8}$$

where $\hat{q}^2 = \hat{u}^2 + \hat{v}^2 + \hat{w}^2$ and $\hat{\ell}$ is the mixing length expressed by East and Sawyer as

$$\frac{\hat{\ell}}{\hat{\delta}_{0.995}} = 0.075\frac{5y}{\hat{\delta}}\left[\left(\frac{5y}{\hat{\delta}}\right)^2 + 1\right]\Big/\left[\left(\frac{5y}{\hat{\delta}}\right)^3 + 1\right] \tag{9}$$

East and Sawyer show very good agreement between measurements and these equations for steady attached adverse-pressure-gradient layers. Simpson et al.[6] show fair agreement in the outer region between their steady freestream data and Eq. (8), using measured mixing lengths. Assuming that $q^2 v \approx q^2 \hat{V}_{re}$, then $\hat{V}_{re}$ is given from Eqs. (6) and (8) as

$$\hat{V}_{re} = \hat{V}|_{\hat{U}=0} - \frac{\partial\hat{\bar{\delta}}_b}{\partial t} = -\frac{0.6\ell}{(\hat{q}^2)^{1/2}}\frac{\partial\hat{q}^2}{\partial y}\Big|_{\hat{U}=0} \tag{10}$$

Because $\hat{w}^2$ measurements for these unsteady flows were not made and Shiloh et al.[26] show that $\bar{w}^2 = \bar{v}^2$ in the outer region, $\hat{q}^2$ was estimated from the approximation $\hat{q}^2 = (\hat{u}^2 + 2\hat{v}^2)$.

Good agreement between calculated and measured values of $\hat{V}_{re}$ was obtained for the $k = 0.61$ unsteady flow, using values

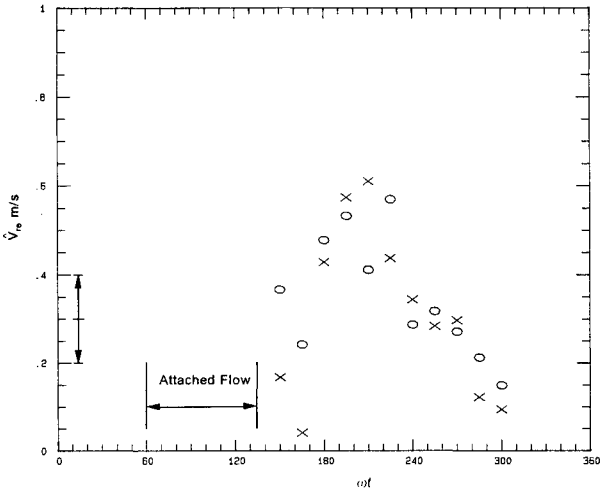

Fig. 11 $\hat{V}_{re}$ **vs** ωt **at** $X = 4.27$ **m,** $k = 0.61$ **(large-amplitude) flow: × = measured; ○ = calculated using Eq. (10) and measured values of mixing length. Typical uncertainty on** $\hat{V}_{re}$ **measured as shown by** $|\leftrightarrow|$.

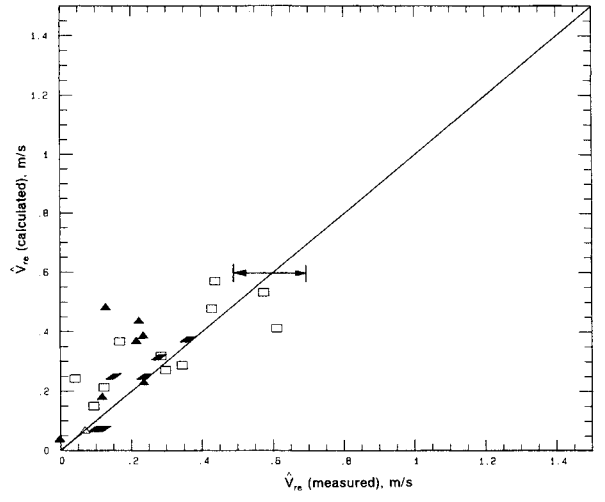

Fig. 12 Correlation between measured and calculated values of $\hat{V}_{re}$ **: △ = 2.95 m; ▲ = 3.51 m; □ = 4.27 m,** $k = 0.61$ **(large-amplitude) flow; ▰, steady flow of Simpson et al.[5] Typical uncertainty on** $\hat{V}_{re}$ **measured as shown by** $|\leftrightarrow|$.

of the mixing length in Eq. (10) calculated from $-\rho\hat{u}v$ and $\hat{U}$ measurements. Results for this flow at 4.27 m are shown in Fig. 11. Data appear to correlate well at all the axial locations for the $k = 0.61$ flow and for the steady flow of Simpson et al.,[5,6] as shown in Fig. 12. However, in the high-frequency $k = 1.03$ and 1.33 unsteady flows, lag between the ensemble-averaged velocity and the turbulence appears to be dominant, and this model overpredicts the $\hat{V}_{re}$. These results indicate that the backflow mass flow rate is controlled by the upstream large eddies in the outer region flow whereas its profile structure is strongly determined by the local flow conditions. This supports the suggestion by Simpson et al.[1,6] that the ensemble-averaged backflow does not appear to come from far downstream but is supplied intermittently by large-scale structures as they pass through the separated region.

Conclusions

All the results presented herein suggest that, in the presence of significant turbulence-energy production near the wall, a normal turbulent boundary-layer type of structure exists for the near-wall phase-ensemble-averaged backflow. Very large backflow velocities appear to be responsible for the production of turbulence energy close to the wall and, in such cases, in addition to the dissipation and diffusion, the production term in the turbulence kinetic energy equation is also important. The skin-friction coefficient, $\hat{C}_f$ in the ensemble-averaged backflow closely correlates on a momentum thickness Reynolds number basis and closely follows the data for zero and mild favorable pressure-gradient-attached turbulent boundary layers, when the data are corrected for the influence of the larger-scale outer region turbulent flow on the near-wall backflow. Simpson's backflow law is valid only in the cases where turbulence-energy production near the wall is negligible, which appears to be a necessary condition for this correlation to hold.

The shapes of the ensemble-averaged mean backflow velocity profiles close to the wall are substantially different in these two cases. In a semilogarithmic plot, the law-of-the-wall velocity profile increases through the viscous sublayer from the wall and then bends over to form a semilog region. For Simpson's correlation, the data in the sublayer and semilog regions follow Eqs. (1) and (2), which show that these two regions blend together tangentially.

Good agreement between measured and calculated values of the re-entrainment velocity of backflow fluid into the outer forward flow region suggests that the backflow volumetric flow rate is determined by the outer part of the upstream flow. The backflow velocity profile shape is governed by the local flow conditions. These are important conclusions and should be included in the calculation methods for separated flows.

Acknowledgments

This work was supported by the U.S. Air Force Office of Scientific Research under Grant 84-0134 and monitored by J. McMichael and Capt. H. Helin.

References

[1] Simpson, R. L.,"Two Dimensional Turbulent Separated Flow," AGARDograph 287, Vol. 1, 1985.

[2] Strickland, J. H., and Simpson, R. L., "The Separating Turbulent Boundary Layer: An Experimental Study of an Airfoil Type Flow," Thermal Fluid Science Center, Southern Methodist Univ., Dallas, TX, Rept. WT-2; also AD-771170/8GA, 1973.

[3] Simpson, R. L., "Interpreting Laser and Hot-Film Anemometer Signals in a Separating Boundary Layer," *AIAA Journal*, Vol. 14, Jan. 1976, pp. 124–126.

[4] Simpson, R. L., "A Model for the Backflow Mean Velocity Profile," *AIAA Journal*, Vol. 21, Jan. 1983, pp. 142, 143.

[5] Simpson, R. L., Chew, Y.-T., and Shivaprasad, B. G., "The Structure of a Separating Turbulent Boundary Layer: Part 1, Mean Flow and Reynolds Stresses," *Journal of Fluid Mechanics*, Vol. 127, 1981, pp. 23–51.

[6] Simpson, R. L., Chew, Y.-T. and Shivaprasad, B. G., "The Structure of a Separating Turbulent Boundary Layer: Part 2, Higher Order Turbulence Results," *Journal of Fluid Mechanics*, Vol. 113, 1981, pp. 53–73.

[7] Simpson, R. L., Shivaprasad, B. G., and Chew, Y.-T., "The Structure of a Separating Turbulent Boundary Layer: Part 4, Effects of Periodic Free-Stream Unsteadiness," *Journal of Fluid Mechanics*, Vol. 127, 1983, pp. 219–261.

[8] Simpson, R. L., and Shivaprasad, B. G., "The Structure of a Separating Turbulent Boundary Layer: Part 5, Effects of Periodic Free-Stream Flows," *Journal of Fluid Mechanics*, Vol. 131, 1983, pp. 319–339.

[9] Simpson, R. L., Agarwal, N. K., Nagabushana, K. A., and Olcman, S., "Spectral Measurements and Other Features of Separating Turbulent Flows," *AIAA Journal*, Vol. 28, March 1990, pp. 446-452.

[10] Dianat M., and Castro I. P., "Measurements in Separating Boundary Layers," *AIAA Journal*, Vol. 27, June 1989, pp. 719–724.

[11] Agarwal, N. K., and Simpson, R. L., "The Structure of Large Amplitude Unsteady Separating Turbulent Boundary Layers," AIAA Paper 87-0191, 1987.

[12] Agarwal N. K., and Simpson, R. L., "Experimental Measurements of the Structure of a Large, Amplitude Unsteady Separating Turbulent Boundary Layers," *Proceedings of AFOSR Workshop II on Unsteady Separated Flows*, Frank J. Seilor Research Laboratory, Rept. FJSRL-TR-88-004, Sept. 1988, pp. 147–153.

[13] Agarwal, N. K., and Simpson, R. L., "Experimental Study of

Unsteady Separating Turbulent Boundary Layers," Aerospace and Ocean Engineering, Virginia Polytechnic, Institute and State University, Blacksburg, VA, Final Technical Report, AFOSR-88-0271TR, Feb. 1988; also AD-A192997.

[14]Agarwal, N. K., and Simpson, R. L., "Separating Turbulent Boundary Layers with Very Large Amplitude Unsteadiness," submitted to *Journal of Fluid Mechanics*, 1989

[15]Agarwal, N. K., and Simpson, R. L.,"A Separating Turbulent Boundary Layer with an Unsteady Diverging Free-Stream," submitted to *Experiments in Fluids*, 1989.

[16]Adams, E. W., and Johnston, J. P., "Flow Structure in the Near-Wall Zone of a Turbulent Separated Flow," *AIAA Journal*, Vol. 26, Aug. 1988, pp. 932-939.

[17]Kays, W. M., and Crawford, M. E., *Convective Heat and Mass Transfer*, 2nd Ed., McGraw-Hill, New York, 1980.

[18]Saripalli, K., and Simpson, R. L., "Investigation of Blown Boundary Layers with an Improved Wall Jet System," NASA CR-3340, 1980.

[19]Patrick W. M., "Flowfield Measurements in a Separated and Reattached Flat Plate Turbulent Boundary Layers," NASA CR-4052, 1987.

[20]Adair D., and Horne, W. C., "Turbulent Separated Flow in the Vicinity of a Single- Slotted Airfoil Flap,"AIAA Paper 88-0613, 1988.

[21]Thompson, B. E., and Whitelaw, J. H., "Characteristics of a Trailing-Edge Flow with Turbulent Boundary-Layer Separation," *Journal of Fluid Mechanics*, Vol. 157, 1985, pp. 305-326.

[22]Ludwieg, H., and Tillmann, W., "Investigation of the Wall-Shearing Stress in Turbulent Boundary Layers," NACA TM-1285, 1950.

[23]Hancock, P. E., and Bradshaw, P., "The Effect of Free-Stream Turbulence on Turbulent Boundary Layers," *Journal of Fluids Engineering*, Vol. 105, 1983, pp. 284-289.

[24]Bradshaw, P., Ferriss, D. H., and Atwell, N. P., "Calculation of Boundary-Layer Development Using the Turbulent Energy Equation" *Journal of Fluid Mechanics*, Vol. 28, 1967, pp. 593-616.

[25]East, L. F., and Sawyer, W. G.,"An Investigation of the Equilibrium Turbulent Boundary Layers," *NATO-AGARD Fluid Dynamics Symposium Proceedings No. 271*, 1979, pp. 6.1-6.19.

[26]Shiloh K., Shivaprasad, B. G., and Simpson, R. L."The Structure of a Separating Turbulent Boundary Layer: Part 3, Transverse Velocity Measurements," *Journal of Fluid Mechanics*, Vol. 131, 1981, pp. 75-90.